applied optics

Intracavity frequency-doubled and single-frequency Ti:sapphire laser with optimal length of the gain medium

HUADONG LU,* XUEJUN SUN, JIAO WEI, AND JING SU

State Key Laboratory of Quantum Optics and Quantum Optics Devices, Institute of Opto-Electronics, Shanxi University, Taiyuan, Shanxi 030006, China
**Corresponding author: luhuadong@sxu.edu.cn*

Received 4 February 2015; revised 31 March 2015; accepted 14 April 2015; posted 14 April 2015 (Doc. ID 233932); published 1 May 2015

A single-frequency 397.5 nm laser by means of an intracavity frequency-doubled Ti:sapphire (Ti:S) laser is presented. In order to obtain the second-harmonic generation with low threshold pump power and high out power, the optimal length of the Ti:S crystal is theoretically analyzed and experimentally measured. The experimental results are in good agreement with the theoretical expectation by comparing the experimental result to the theoretical value of the threshold pump power. After inserting the nonlinear BIBO and LBO crystals, the obtained output powers of the 397.5 nm laser are 1.58 and 0.78 W, respectively. Lastly, the tuning characteristic, power stability, and beam quality are also discussed. © 2015 Optical Society of America

OCIS codes: (140.3460) Lasers; (140.3515) Lasers, frequency doubled; (140.3560) Lasers, ring; (140.3570) Lasers, single-mode.

http://dx.doi.org/10.1364/AO.54.004262

1. INTRODUCTION

Continuous-wave (CW) coherent light sources in the blue to near-ultraviolet (UV) spectral region are useful for applications in biomedicine, metrology, high-resolution spectroscopy, atom trapping, and quantum optics. In the UV spectrum, for instance, the cooling transmission of $^{40}Ca^{2+}$ ions ($S_{1/2}$-$P_{1/2}$) falls within the wavelength of 397.5 nm [1]. In quantum optics experiments, single-frequency 397.5 nm lasers can be used as the pump sources of the optical parametric oscillators and amplifiers, which are the important devices for the generation of optical squeezed states and entangled states at the wavelength of 795 nm. The generated 795 nm nonclassical states of light can be applied in the advanced experimental investigations of information protocols and quantum communication because the 795 nm corresponds to the D_1 line of rubidium (Rb) [2]. In order to generate a CW squeezed vacuum state resonant on the Rb D_1 line, Tanimura *et al.* [3] utilized an external power-enhancement cavity doubling of a Ti:sapphire (Ti:S) laser to obtain a 105 mW single-frequency 397.5 nm laser, which was used as the pump source of the squeezed vacuum state and observed a squeezing level of −2.75 dB. In 2007, Hetet *et al.* [4] implemented the 5 dB of quantum noise suppression. Recently, Han *et al.* realized a 397.5 nm tunable laser with output power of 130 mW via ring-cavity-enhance frequency doubling [5]. In these experiments, the external frequency doublers of the Ti:S lasers have to be locked to the input laser frequency to obtain stable single-frequency 397.5 nm laser, which increases the complexity of the laser system and decreases the stability of the laser system. Compared to the external frequency doubler, the intracavity second-harmonic generation (SHG) by inserting a nonlinear crystal into the single-frequency Ti:S laser resonator is an attractive approach to realize the blue to near-UV output. In 2003, White *et al.* [6] realized a tunable single-frequency UV laser generated from a CW Ti:S laser with an intracavity periodically poled lithium niobate crystal. The maximal second-harmonic power of 114 mW was measured at 403 nm, but instability in the UV output power and the reduction in second-harmonic power at shorter wavelengths were observed. In 2007, Cruz and Cruz [7] reported on CW SHG of infrared Ti:S lasers using nonlinear BIBO (Bismuth Triborate, BiB_3O_6) crystal in an external power-enhancement cavity and inside the laser resonator. The obtained powers are 70 and 266 mW of single-frequency radiation at 423 nm for external frequency doubler and intracavity SHG, respectively. In 2011, Li *et al.* [8] realized a single-frequency tunable 461 nm laser with output power of 280 mW by employing the same schematic as [7]. So far, there are few reports on the intracavity frequency doubling of the single-frequency Ti:S laser below the wavelength of 400 nm since the absorption in the UV spectrum region of lots of nonlinear crystals is strong, especially in the range of <400 nm. So we must optimize the laser resonator and the parameters of the crystals to decrease the intracavity losses and choose the appropriate nonlinear crystal to obtain a single-frequency UV laser with high output power. In this

paper, we first analyze the optimal length of the active Ti:S crystal in a single-frequency resonator with an intracavity nonlinear crystal for SHG to decrease the intracavity loss and achieve the lowest threshold pump power. Then, by employing the theoretical length of the optimal Ti:S crystal, an astigmatism compensated resonator is designed and constructed. At last, by inserting nonlinear BIBO and LiB_3O_5 (LBO) crystal, we achieve a single-frequency 397.5 nm laser with the output power up to 1.5 and 0.8 W, respectively. To the best of our knowledge, these are the highest output powers for intracavity frequency-doubled Ti:S lasers. The experimental observation of the threshold pump power and the theoretical calculation are in good agreement, which provides us a feasible way to choose the length and the absorption coefficient of the Ti:S crystal to achieve a UV laser with low threshold pump power and high output power.

2. THEORETICAL ANALYSIS

Ti:S crystal is an unusual laser medium because of its broad coverage of the near-infrared spectral region. However, the parasitic absorption [9] in the material often badly influences the conversion efficiency of the laser. This phenomenon has been attributed to the presence of Ti^{4+} ions in the crystal (the active ion is Ti^{3+}). The crystal quality is characterized in terms of an absorption figure of merit (FOM) defined as the ratio of the absorption at the pump laser wavelength to the parasitic absorption at laser wavelength (FOM $= \alpha/\alpha_l$, where α and α_l are the absorption coefficients of the Ti:S crystal at the pump laser wavelength and the laser wavelength, respectively) [10]. The higher the Ti concentration is, the lower the value of the FOM is and the stronger the parasitic absorption of the Ti:S crystal at laser wavelength is. This is a focus to design an intracavity frequency doubling Ti:S laser with high output power. As usual, the Ti:S crystal with low Ti concentration is used in the experiment in order to avoid the absorption of the crystal at laser wavelength. However, low concentration can decrease the absorption of the crystal at the pump laser. So, there is an optimal length of the Ti:S crystal to make the laser obtain the largest output power for doubling-frequency laser when the Ti concentration is given.

Laser performance can be analyzed by using a two-dimensional model for a longitudinally pumped system in which both lasers are assumed to operate in a fundamental Gaussian mode. The CW threshold power P_{th} is given by the following equation [11]:

$$P_{\text{th}} = \frac{1}{\eta_t}\frac{\pi h\upsilon_p}{2\sigma\tau}(L_{\text{cav}} + L_{xtl})(\omega_0^2 + \omega_p^2)[1 - \exp(-\alpha l)]^{-1}, \quad (1)$$

where η_t is the transmission efficiency of the pump laser, $h\upsilon_p$ is the pump photon energy, σ is the emission cross section, τ is the upper-state lifetime. ω_0 and ω_p are the cavity-mode and pump radii in the crystal, respectively. The final term in brackets represents the pump-absorption efficiency (α is the absorption coefficient at υ_p and l is the crystal length). L_{cav} and L_{xtl} are round-trip cavity loss and the loss caused by the parasitic absorption of the crystal, respectively. The loss caused by the parasitic absorption in the crystal is given by

$$L_{xtl} = 1 - \exp\left(\frac{-\alpha l_{\text{eff}}}{\text{FOM}}\right), \quad (2)$$

where l_{eff} is the effective parasitic absorption length, which equates l in the traveling-wave cavtiy and $2l$ in the standing-wave cavity, respectively. Substituting Eq. (2) into Eq. (1), the relation for the threshold pump power and the length of the Ti:S crystal is obtained. Figure 1 is the functions of the threshold pump power versus the length of the Ti:S crystal for three different absorption coefficients at the pump laser wavelength, in which the experimentally measured parameters for our laser system, $\upsilon_p = c/\lambda_p$, $\lambda_p = 532$ nm, $\eta_t = 95\%$, $\sigma = 4.9\times 10^{-20}$ cm^2, $\tau = 3.15$ μs, $L_{\text{cav}} = 3.88\%$, $\omega_0 = 36$ μm, $\omega_p = 30$ μm, and FOM $= 200$ are utilized. We can see there is an optimal $l = l_{\text{opt}}$ for a given α, where the threshold pump power reaches to the lowest point, and l_{opt} decreases when α increases. The optimal length of the Ti:S crystal can be obtained when

$$\frac{dP_{\text{th}}}{dl} = 0. \quad (3)$$

For the Ti:S crystal with the absorption coefficient of 1.15 cm^{-1} and the experimental parameters of our laser system above mentioned, we can see that the optimal length of the Ti:S crystal is 21 mm and the pump power at threshold is 4.9 W.

3. EXPERIMENTAL SETUP

According to the theoretical analysis, we design an all-solid-state CW single-frequency Ti:S laser with an intracavity frequency doubler, which is shown in Fig. 2. The pump source is a single-frequency and frequency-doubled Nd:YVO_4 laser with a maximal 20 W power of the green laser (F-VIII B, Yuguang Co., Ltd.) [12]. The pump green laser guided by M_1 and M_2 is coupled into the resonant cavity of the Ti:S laser by a telescope coupling system, which consists of two lenses f_1 and f_2 with the focal lengths of 200 and 120 mm, respectively. The half-wave plate in front of the resonator is used for the polarization alignment of the pump laser with respect to the optical axis of the Ti:S crystal. An astigmatism compensated doubled-folded resonator is employed to give two tight-focus

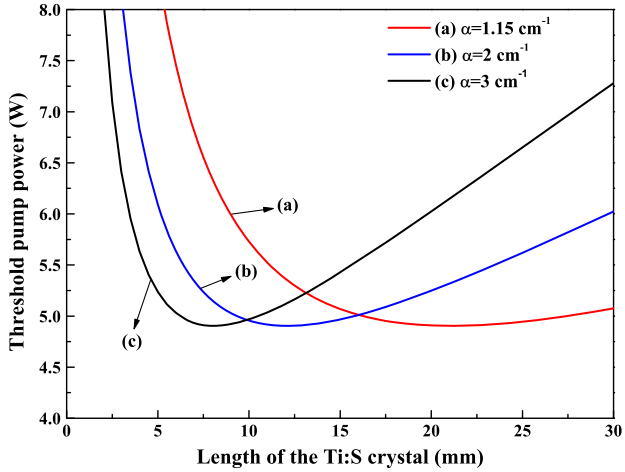

Fig. 1. Threshold pump power versus the length of the Ti:S crystal.

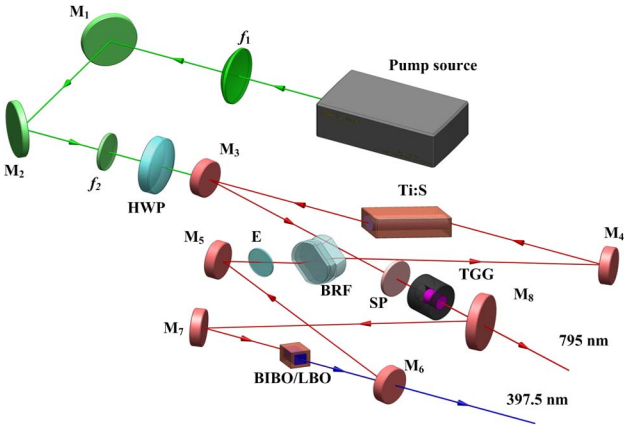

Fig. 2. Schematic diagram of the intracavity frequency-doubled and single-frequency Ti:S laser.

regions: one is for the Ti:S crystal and the other is for the frequency doubler. The ring-type configuration is composed of two curved mirrors with a 100-mm radius of curvature (M_3 and M_4), two curved mirrors with a 50-mm radius of curvature (M_6 and M_7), and two flat mirrors (M_5 and M_8). M_3 and M_4 are coated with high-reflection (HR) films at 750–820 nm and antireflection (AR) films at 532 nm, and the folding angle at M_3 and M_4 is set to 15.8°. M_5 is coated with HR films at 750–820 nm. Another two curved mirrors (M_6 and M_7) are coated with HR films at 750–850 nm and AR films near 398 nm, and the folding angle at M_6 and M_7 is set to 10°. The angles of four concave mirrors can be enough to compensate the astigmatism in the ring cavity induced by the Brewster-cut intracavity elements, including Ti:S gain crystal, a three-plate birefringent filter (BRF), and an optical diode [13,14]. The Brewster-angle-cut (60.4°) Ti:S crystal with a 4-mm diameter is utilized. The absorption coefficient at the pump wavelength of 532 nm and FOM are 1.15 cm^{-1} and about 200, respectively. The optimal length of the Ti:S crystal is 21 mm according to the above analysis, which is used in the experiment and mounted in a closed copper block oven cooled by water circulation and positioned between M_3 and M_4. The three-plate BRF with thickness of 1, 2, and 4 mm is inserted into the resonator with its Brewster incidence angle (57°) for coarsely and broadband frequency tuning. To enforce unidirectional oscillation, an optical diode based on the Faraday effect is used. It comprises a Brewster-cut, 3-mm long, terbium gallium garnet (TGG) Faraday crystal placed inside a stack of permanent Sm-Co ring magnets. A thin quartz plate is used to compensate, via optical activity, the polarization rotation induced by the TGG crystal.

Although the optimal length of the Ti:S crystal can make the laser achieve a low absorbed pump power at threshold, we should also consider how to obtain a higher output power by choosing the appropriate nonlinear crystal for the intracavity frequency doubling. For SHG below 400 nm, crystal candidates are LBO, beta barium borate (BBO), BIBO, lithium iodate ($LiIO_3$), and periodically poled $KTiOPO_4$ (PPKTP). Compared to BBO and $LiIO_3$, LBO has a much smaller walk-off angle and BIBO has higher nonlinearity and very good optical quality with low scattering and absorption losses.

Table 1. Parameters of the BIBO and LBO Crystals

Crystal	L × W × H	θ (°)	ϕ (°)	d_{eff} (pm/V)	ρ (mrad)
LBO	8 × 3 × 3	90	32.1	0.745	16.64
BIBO	5 × 3 × 3	150.7	90	3.73	60.01

Though PPKTP has advantages such as being free of walk-off and high nonlinearity, the strong absorption below 400 nm limits its application in the high-power UV generation [15]. So, in the experiment, a LBO and a BIBO crystal are inserted into the resonator to be as the frequency doubler, respectively. The parameters are listed in Table 1:

From the table, we can see the type-I phase-matched BIBO crystal has a much higher nonlinear coefficient than that of LBO (lithium triborate, LiB_3O_5), but the walk-off angle (ρ) of the BIBO is larger than that of the LBO. To realize SHG of the 795 nm laser, LBO and BIBO are cut on type-I critically phase-matched angle that is $\theta = 90.0°$, $\Phi = 32.1°$ and $\theta = 150.7°$, $\Phi = 90°$, respectively. Both crystals are wrapped with an indium foil and mounted in a temperature-controlled copper oven. Using a thermoelectrical temperature controller with accuracy of 0.03 K, the temperature of the LBO and BIBO crystal is stabilized to the optical phase-matching temperature value of 300 K.

4. EXPERIMENTAL RESULTS

The function curve of the output power for the single-frequency 397.5 nm laser versus the pump power is plotted in Fig. 3. When the frequency doubler is BIBO, the maximum output power of 1.58 W is measured under the pump power of 20.2 W, which is the maximal output power of the pump source. The threshold pump power and the optical-optical conversion efficiency (from 532 to 397.5 nm) are 5.1 W and 7.8%, respectively. The longitudinal-mode structure is monitored by a scanned Fabry–Perot cavity (F-P-100, Yuguang Co., Ltd.) and the transmission curve is shown in Fig. 4. The free spectrum range and the finesse (f) of the F-P cavity are 750 MHz

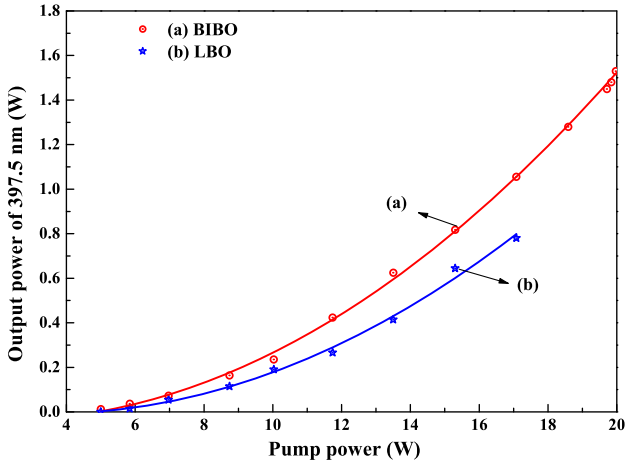

Fig. 3. Output power of Ti:S laser at 397.5 nm as a function of the pump power.

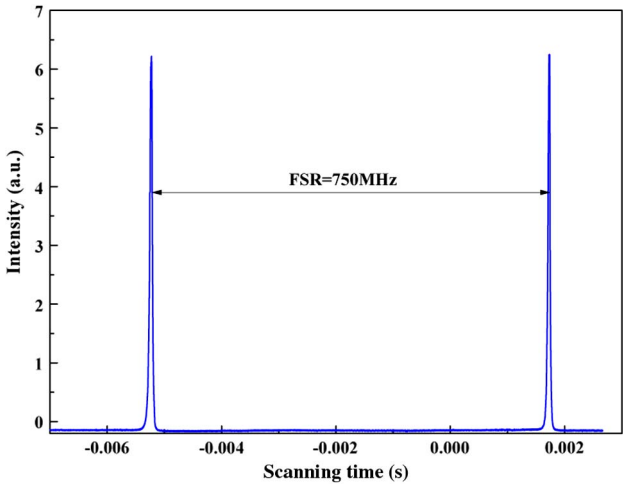

Fig. 4. Laser transmission intensity obtained by scanning a confocal F-P cavity.

and 150, respectively. It demonstrates that the laser works with single-frequency operation, which is owing to the existence of the nonlinear loss introduced by the nonlinear crystal [16]. Though the laser has high output power and optical-optical conversion efficiency, the instability of the output power is observed. After a few minutes, the second-harmonic power reduces to a quite smaller value, which is similar to the phenomenon mentioned in [7]. We also observed that the higher power can be recovered by rotating the BRF to realize the frequency tuning of the laser. It indicates that the generation of the UV laser with the high output power can change the phase-matching condition of the BIBO, which is defined as the photorefractive effect. In addition, because of the large walk-off effect, the emitted UV beam is elliptical in shape, and there are several interference fringes mixed in the output beam. When the frequency doubler BIBO is replaced by the LBO, the output power is only 0.78 W at the pump power of 17.08 W with the threshold power of 5.1 W. The optical-optical conversion efficiency (from 532 to 397.5 nm) is 4.6%, which is limited by the nonlinear conversion coefficient and the length of the nonlinear LBO crystal. When the pump power is higher than 17.08 W, the output power of the 397.5 nm laser decreases since the low nonlinear coefficient of the LBO make the laser reach the gain saturation. The measured threshold pump power of 5.1 W in the experiment for LBO and BIBO is in good agreement with the theoretical calculation (4.9 W), which shows that 21 mm is the optimal length of the Ti:S crystal. The long-term power stability of the laser recorded by a power meter is shown in Fig. 5. The power stabilities of the laser with the LBO as the frequency doubler is better than ±3.2%. The phenomenon such as the output power reduced to a small value is not observed when the LBO acts as the frequency doubler, which indicates the difference of the LBO and BIBO crystals. The tuning characteristic of the UV laser is implemented by rotating the BRF when the frequency doubler is LBO. Because of the phase-matching range of the LBO, the tuning of the UV laser is limited to the range from 394 to 402 nm, as shown in Fig. 6. Though the emitted UV beam is elliptical in

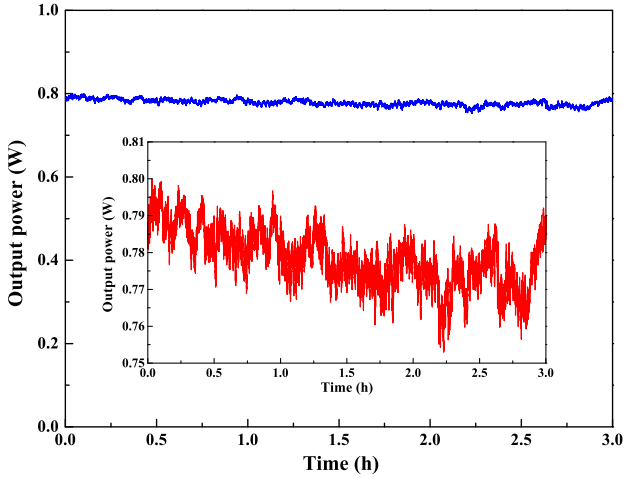

Fig. 5. Power stability of the UV laser in 3 h.

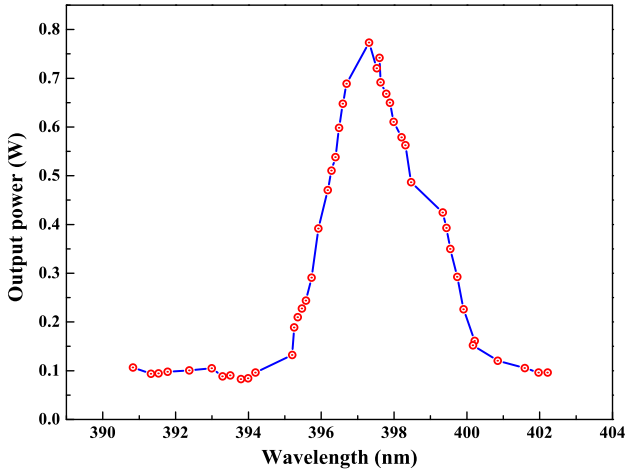

Fig. 6. Tuning characteristic of the UV laser.

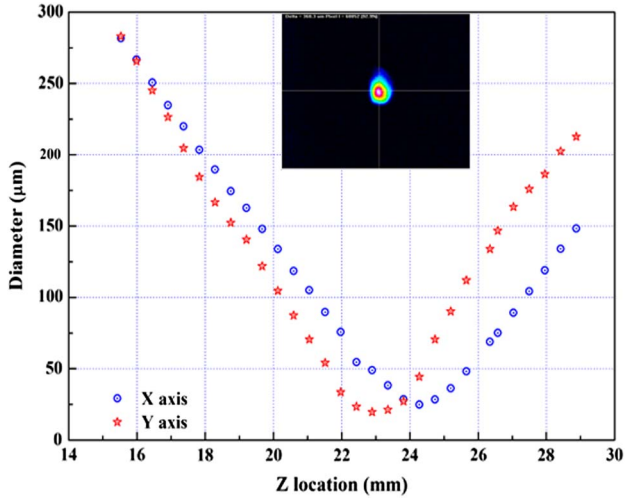

Fig. 7. Measured M^2 values and the spatial beam profile for a 397.5 nm laser.

shape, there are not interference fringes mixed in the UV laser beam. By using a pair of cylindrical lenses with the focal lengths of 50 mm to shape the UV laser beam, the high beam quality of the laser is obtained. The beam quality of the laser is measured by a M^2 meter (M2SET-VIS, thorlabs), and the values of M_x^2 and M_y^2 are 1.48 and 1.18, respectively. The measured caustic curve and the corresponding spatial beam profile are shown in Fig. 7 and its inset, respectively.

5. CONCLUSIONS

In summary, a single-frequency and intracavity frequency-doubled Ti:S laser with low threshold pump power and high output power is presented. We theoretically analyze the dependence of the threshold pump power of the laser on the length of the Ti:S crystal and obtain the optimal length of the Ti:S crystal. The experimental measurements are in good agreement with the theoretical expectation. By inserting the BIBO and LBO crystals, respectively, the single-frequency 397.5 nm lasers with output powers of 1.58 and 0.78 W are obtained. The tuning characteristic, power stability, and beam quality are also discussed. For the first time, we realize a single-frequency 397.5 nm laser with intracavity frequency doubling Ti:S laser. The obtained single-frequency 397.5 nm laser can be used in the generation of the entangled states at the wavelength of 795 nm, which corresponds to the D_1 line of the Rb atoms.

National Natural Science Foundation of China (61227015, 61227902, 61405107); Natural Science Foundation of Shanxi (2014021011-3); Scientific and Technological Innovation Programs of Higher Education Institutions in Shanxi (2013104).

REFERENCES

1. J. Eschner, G. Morigi, F. Schmidt-Kaler, and R. Blatt, "Laser cooling of trapped ions," J. Opt. Soc. Am. B **20**, 1003–1015 (2003).
2. Z. X. Xu, Y. L. Wu, L. Tian, L. R. Chen, Z. Y. Zhang, Z. H. Yan, S. J. Li, and H. Wang, "Long lifetime and high-fidelity quantum memory of photonics polarization qubit by lifting zeeman degeneracy," Phys. Rev. Lett. **111**, 240503 (2013).
3. T. Tanimura, D. Akamatsu, Y. Yokoi, A. Furusawa, and M. Kozuma, "Generation of a squeezed vacuum resonant on a rubidium D_1 line with periodically poled $KTiOPO_4$," Opt. Lett. **31**, 2344–2346 (2006).
4. G. Hetet, O. Glockl, K. A. Pilypas, C. C. Harb, B. C. Buchler, H. A. Bachor, and P. K. Lam, "Squeezed light for bandwidth-limited atom optics experiments at the rubidium D_1 line," J. Phys. B **40**, 221–226 (2007).
5. Y. S. Han, X. Wen, J. D. Bai, B. D. Yang, Y. H. Wang, J. He, and J. M. Wang, "Generation of 130 mW of 397.5 nm tunable laser via ring-cavity-enhanced frequency doubling," J. Opt. Soc. Am. B **31**, 1942–1947 (2014).
6. R. T. White, I. T. Mckinne, S. D. Butterworth, G. W. Baxter, D. M. Warrington, P. G. R. Smith, G. W. Ross, and D. C. Hanna, "Tunable single-frequency ultraviolet generation from a continuous-wave Ti:sapphire laser with an intracavity PPLN frequency doubler," Appl. Phys. B **77**, 547–550 (2003).
7. L. S. Cruz and F. C. Cruz, "External power-enhancement cavity versus intracavity frequency doubling of Ti:sapphire lasers using BIBO," Opt. Express **15**, 11913–11921 (2007).
8. F. Q. Li, Z. Shi, Y. M. Li, and K. C. Peng, "Tunable single-frequency intracavity frequency-doubled Ti:sapphire laser," Chin. Phys. Lett. **28**, 124205 (2011).
9. P. F. Moulton, "Spectroscopic and laser characteristics of $Ti:Al_2O_3$," J. Opt. Soc. Am. B **3**, 125–133 (1986).
10. J. F. Pinto, L. Esterowitz, G. H. Rosenblatt, M. Kokta, and D. Peressini, "Improved Ti:sapphire laser performance with new high figure of merit crystals," IEEE J. Quantum Electron. **30**, 2612–2616 (1994).
11. J. Harrison, A. Finch, D. M. Rines, and P. F. Moulton, "Low-threshold, cw, all-solid-state $Ti:Al_2O_3$ laser," Opt. Lett. **16**, 581–583 (1991).
12. Q. W. Yin, H. D. Lu, and K. C. Peng, "Investigation of the thermal lens effect of the TGG crystal in high-power frequency-doubled laser with single frequency operation," Opt. Express **23**, 4981–4990 (2015).
13. Y. Sun, H. D. Lu, and J. Su, "Continuous-wave, single-frequency, all-solid-state $Ti:Al_2O_3$ laser," Acta Sinica Quantum Opt. **14**, 344–347 (2008).
14. H. D. Lu, X. J. Sun, M. H. Wang, J. Su, and K. C. Peng, "Single frequency Ti:sapphire laser with continuous frequency-tuning and low intensity noise by means of the additional intracavity nonlinear loss," Opt. Express **22**, 24551–24558 (2014).
15. G. Hansson, H. Karlsson, S. H. Wang, and F. Laurell, "Transmission measurements in KTP and isomorphic compounds," Appl. Opt. **39**, 5058–5069 (2000).
16. H. D. Lu, J. Su, Y. H. Zheng, and K. C. Peng, "Physical conditions of single-longitudinal-mode operation for high-power all-solid-state lasers," Opt. Lett. **39**, 1117–1120 (2014).